

An Integrated Array Antenna for a TES Imaging Radiometer: General Concept and Simulations

Sergey V. Shitov, Alexander N. Vystavkin, *Member, IEEE*

Abstract—We are developing an imaging radiometer based on concept of direct connection of superconducting TES detector to a planar antenna. To control a large-dimension imaging array, multiplexing procedure via method of projection is suggested; the antenna array and the image are rotating reciprocally in their common plane during the signal integration process. Each crossed double-slot antenna feeds two TES detectors integrated in the central part of the antenna via a combination of microstrip and coplanar transmission lines. The instantaneous bandwidth of 50% is estimated for 5- Ω TES detector tuned at 600 GHz. The coupling circuit with overlapping RF feed-lines demonstrated cross-talk interference below -30 dB. Infinite expansion of the array is possible while the number of output leads can be minimized to $N+M$ for N by M array; the continuous signal integration is available for all pixels. The design and analysis are performed using commercial EM-software.

Index Terms—Bolometer, imaging array, method of projection, slot antenna, transition edge sensor.

I. INTRODUCTION

A superconducting transition-edge sensor (TES) bolometer [1]-[3] consists of a radiation absorbing element attached to a superconducting film with a transition temperature T_c , which is weakly coupled to a heat sink at temperature $T_0 \approx T_c/2$. The superconducting film is heated by a bias source to an operating point within superconducting transition, where its resistivity is very sensitive to temperature changes. Since the bias voltage is fixed, the bias current through the TES is temperature-sensitive (optical signal sensitive), and it can be coupled to an ultra-low-noise amplifier based on a superconducting quantum interference device (SQUID amplifier).

Manuscript received May 2, 2005. This work was supported in parts by the by Russian State Program "Support of Leading Scientific Schools in Russia" (grant 1548.2003.2) and Program for Basic Research "Problems of Radio Physics" (Department of Physical Sciences, Russian Academy of Science) in direction "Applications in Terahertz Range".

S. V. Shitov is now with the National Astronomical Observatory of Japan, Mitaka, Tokyo 181-8588, Japan, on leave from the Institute of Radio Engineering and Electronics, Russian Academy of Sciences, Moscow 125009, Russia (phone: +81-422-34-3629; fax: +81-422-34-3817; e-mail: sergey@alma.mtk.nao.ac.jp, sergey@hitech.cplire.ru).

Alexander N. Vystavkin is with the Institute of Radio Engineering and Electronics, Russian Academy of Sciences, Moscow 125009, Russia (e-mail: vyst@hitech.cplire.ru).

The voltage bias introduced by Irwin [4] provides a negative electrothermal feedback, which stabilizes the temperature of the TES at the operating point on the transition. The electrothermal feedback keeps the total power input constant. This negative-feedback TES bolometer has advantages of good linearity and wider bandwidth; they can be produced by thin-film deposition and optical lithography, so they are suitable for large format arrays.

The absorption of RF power can be realized either directly within radiation absorption pads [5]-[10] or via combination of antennas and transmission lines heating the absorber. The antenna-coupled TES bolometer development [11]-[15] is just beginning, and it still tends to employ traditional thermally isolating legs or very thin membranes. Fortunately, the small area of integrated antenna terminations makes possible using TES absorber directly deposited on the silicon substrate without any legs for thermal isolation. At temperatures 0.1 K, the weakness of the electron-phonon interaction impedes the flow of heat from the metal into the dielectric substrate and can provide values of thermal conductance that are appropriate for low-background astronomical bolometers.

In our antenna-integrated TES, similar to [16]-[18], the extra weakening of the electron-phonon interaction is assumed via Andreev electron-reflection effect at the interface between the submicron-size absorber and leads of the antenna made from a higher- T_c superconductor (Nb). For our Mo/Cu absorber ($T_c = 0.1-0.3$ K) [19] operating within its superconductor transition region, the RF current from antenna assumed to be the source of hot electrons within the absorber. The heat escape from the absorber is limited by the above-mentioned Andreev mirrors, and the goal of producing bolometers with $NEP \approx 10^{-18}$ W Hz^{1/2} and below can be set.

To control a large-dimension imaging array, the multiplexing procedure via method of projection, when the array and the radiation source image are rotating reciprocally in their common plane, is suggested [20]. Since the sky objects usually emit both polarizations, the projections method needs both polarizations to be analyzed. To receive both polarizations independently, a crossed double-slot antenna (CDSA) is used [21], but unlike in [15], we assume direct connection of TES to the leads of antenna.

To read and amplify output signals from the array, a concept of SQUID-amplifier working in a frequency

multiplexing mode [22] is being developed as a part of the imaging array research. The method of projections allows for minimizing the number of output leads to $N + M$ for $N \times M$ array, since it assumes the connection of all detectors within a row and a column in parallel for their bias voltages and output currents. To resolve a 2-D image, the rotation of the image in respect to the array is assumed using, for example, a K-mirror system. Note that a full-time signal accumulation is possible for all elements of the imaging array.

Present paper describes our approaches for designing a practicable array antenna, which can work with TES detectors at submillimeter wavelength.

II. DETAILS OF DESIGN

A. Antenna Packaging

The distance between elementary antennas can be found using requirements for their beams' overlapping. The beams' overlapping level can be defined according to desired sampling technique. We have chosen the under-sampling factor of four that allow the space between neighboring beams is just enough for accommodating another beam. This means that complete mapping of the image can be achieved via two samplings for each axis: to fill in a 2-D image four samplings are needed. The intersection level (taper level) is chosen at about -10 dB for two reasons. 1) Such low taper allow for clear separation of two neighboring pixels of the image, which has high pixel-to-pixel contrast. 2) High taper (say, -3 dB) means direct (on-chip) interference (cross-talk) of the integrated antennas via common RF currents that is in contrary with the wish of high-resolution imaging. Fig. 1 presents the antenna package with separation of 2λ (center-to-center) that provide low cross-talk between all components of the array as shown in Fig. 2. The extremely low cross-talk between the two polarizations of a crossed double-slot antenna (CDSA) is illustrated in Fig. 3 via the visualization of the current density distribution.

B. RF Coupling Circuit and DC Interconnections

Each pixel of the array contains two coupling circuits feeding two TES detectors integrated in the central part of the CDSA. These two circuits must overlap as shown in Fig. 3. Since the polarization separation properties of the two antennas (of the CDSA), each detector is sensing only one polarization. To connect each slot-antenna to its own TES detector, the combination of microstrip and coplanar waveguides is used. Since the output impedance of a slot antenna is about 50Ω that is essentially higher than the resistance of the TES detector ($0.5-5 \Omega$), a careful impedance transformation has to be considered. We have found that the problem of RF coupling of the low-resistive TES detectors is somewhat similar to the well-known problem of coupling SIS detectors [3]. The impedance of a small (low-resistive) TES is presumably reactive (inductive), and it needs to be tuned with a capacitive tuner, which can be provided by

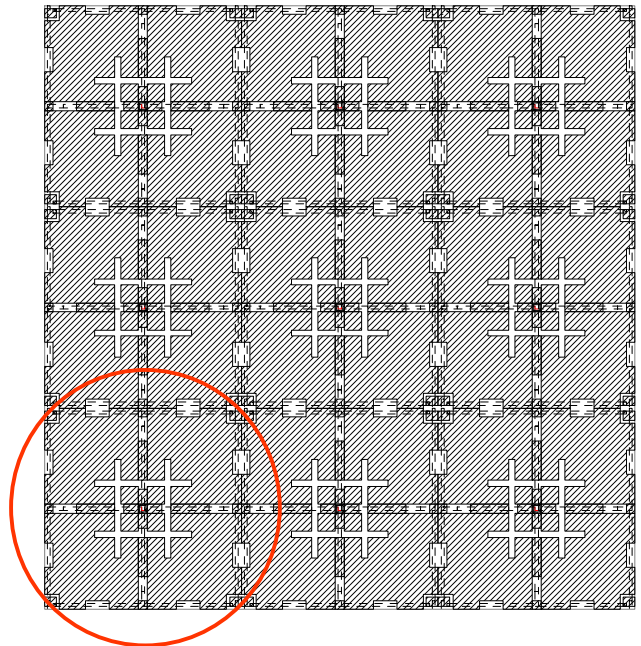


Fig. 1. Layout of array antenna. Each crossed double-slot antenna provides an elementary cell (pixel) marked by circle. Infinite multiplication is possible while keeping same complexity of the wiring.

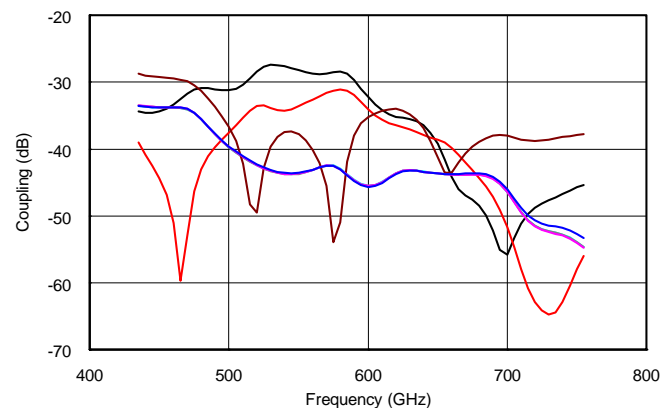


Fig. 2. Parasitic coupling between neighboring antenna elements of the array from Fig. 1. Simulation performed for CDSA positioned in the corner of the chip.

a fraction of a microstrip line ($L < \lambda/4$). We have estimated the bandwidth of about 50% for a 5-Ohm TES detector tuned for central frequency 600 GHz as shown in Fig. 4. Note that a narrower RF bandwidth (narrow-band filtering) can be provided simply via extra inductance in series with TES that result in higher Q-factor of the circuit.

To achieve the best symmetry on the two detector circuits, their overlapping is arranged on the base of coplanar waveguide (CPW) that allow for using only two metal layers as shown in Fig. 5. The CPW solution helps to minimize the asymmetry of the detectors in respect to the ground plane. In spite heavy cross-talk interference between overlapping CPW lines looks highly probable, we estimated the cross-talk below -30 dB at 600 GHz as presented in Fig. 6. Extra measures

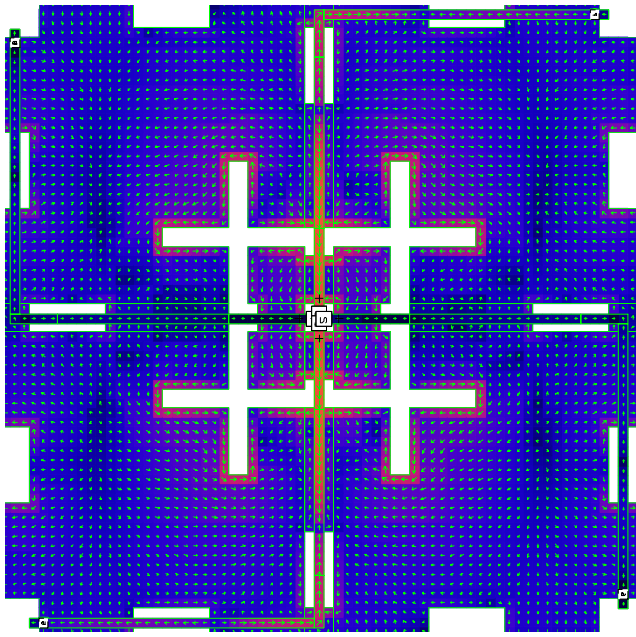


Fig. 3. RF currents at 600 GHz for the cell-antenna from Fig. 1 (simulation). Red and blue colors present high and low current density accordingly. Microstrip lines in the wiring layer provide both RF coupling and DC filtering.

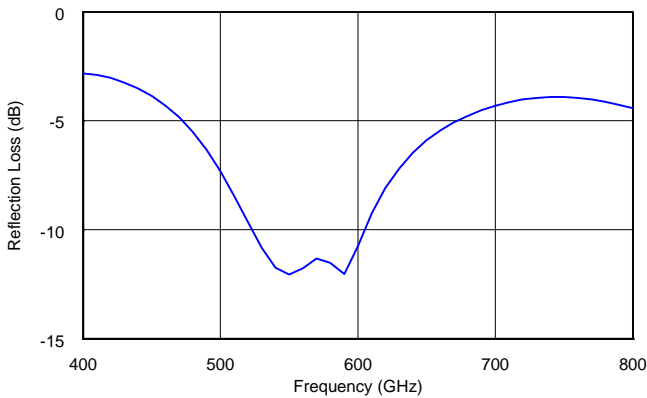


Fig. 4. Simulation of antenna coupling with 5-Ohm TES bolometer.

can be taken for further reducing of the cross-talk as illustrated in Fig. 5 and Fig. 6.

The DC filters of the antennas (RF band-stop filters) are designed using alteration of $\lambda/4$ -long CPW and microstrip waveguides that is clearly seen in Fig. 3. The CPW lines are formed by opening $\lambda/4$ -long holes in the ground plane of the microstrip lines. The extensions of the RF filters at horizontal and vertical directions (see Fig. 3) form the DC bias/output signal wires, which are connecting all detectors in parallel for each column and for each row of the antenna array. This allow for virtually infinite expansion of number of pixels in the array without essential growing of complexity of the DC bias/read-out circuit. The presented simulations, including the antennas' impedance, are performed using commercial 2.5-D electromagnetic software ("Microwave Office" [23]).

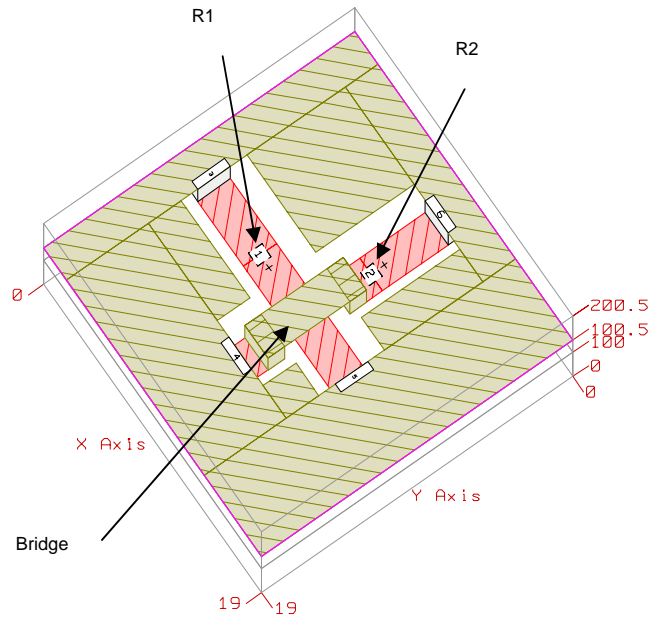


Fig. 5. Design of cross-line region providing best cross-talk isolation; internal ports R1 and R2 stand for two TES-detectors. Absolute symmetry of the structure is not possible, since detectors cannot be fabricated on top of each other.

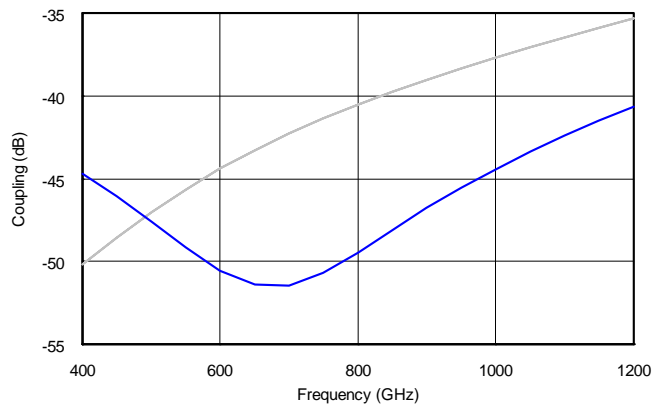


Fig. 6. Cross-talk level for the overlapping RF circuits from Fig. 5 (simulation). Result of improvement in cross-talk isolation at about 600 GHz is presented by the two curves that achieved via careful design of the asymmetric cross-hole as shown in Fig. 5.

C. Optical System and Cryostat

It is known that most of planar antennas are the low-gain antennas which have a very broad beam (typically wider than 90 degrees). To couple such antennas to the high-gain telescope beam, an intervening optics is necessary. The most advanced techniques of printed antennas employ the immersion-type lenses: hyper-hemispherical or truncated elliptical lenses [24]. It is important that the elliptical lens can work in the diffraction limit. This means it can offer the ultimate gain providing the beam waist at its aperture. Fig. 7 presents the optical concept for the integrated antenna array from Fig. 1 placed on the back of a truncated ellipsoid. We are going first try a small 9-pixel array of 3 by 3 pixels. To

achieve low spherical aberrations, the diameter of ellipsoid is estimated as 25 mm for our case.

To reduce the heat load to the milli-Kelvin stage and the detector, the infra-red (IR) filters are necessary along with proper focusing of the array beam at the smallest possible apertures of the thermal shields of the cryostat. The pure mono-crystalline silicon is a good material for both low-loss terahertz optics and efficient IR filters. The preliminary design concept shown in Fig. 7 assumes two long-focusing silicon lenses as the intervening optics in combination with three additional IR filters (scattering filters of narrow-band mesh filters).

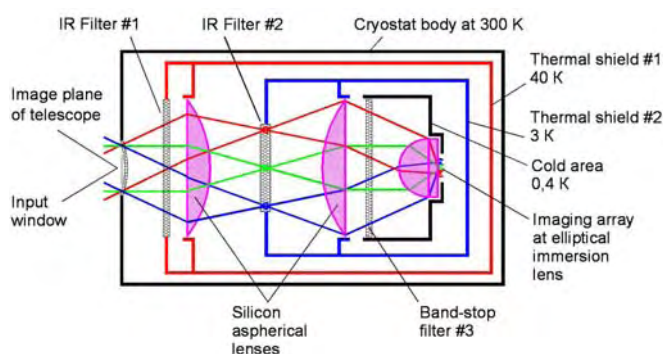


Fig. 7. Optical scheme of the imaging array TES-radiometer mounted within the ultra-low temperature cryostat.

ACKNOWLEDGMENT

Authors thank B. Karasik, H. Matsuo and M. Ishiguro for fruitful discussions.

REFERENCES

- [1] P. L. Richards, "Bolometric detectors for space astrophysics," in *Proc. Far-IR, Sub-MM, and MM Detector Workshop*, vol. NASA/CP-2003-211 408, J. Wolf, J. Farhoomand, and C. R. McCreight, Eds., 2003, pp. 219–223.
- [2] P. L. Richards, C. R. McCreight, "Infrared detectors for astrophysics," *Physics Today*, February 2005, pp. 41–47.
- [3] J. Zmuidzinas, P. L. Richards, "Superconducting detectors and mixers for millimeter and submillimeter astrophysics," *Proc. IEEE*, 2004, v. 92, pp. 1597–1616.
- [4] K. Irwin, "An application of electrothermal feedback for high-resolution cryogenic particle-detection," *Appl. Phys. Lett.*, vol. 66, no. 15, pp. 1998–2000, 1995.
- [5] J. Gildemeister, A. Lee, and P. Richards, "Monolithic arrays of absorber-coupled voltage-biased superconducting bolometers," *Appl. Phys. Lett.*, vol. 77, no. 24, pp. 4040–4042, 2000.
- [6] D. J. Benford, G. M. Voellmer, J. A. Chervenak, K. D. Irwin, S. H. Moseley, et al., "Thousand-element multiplexed superconducting bolometer arrays," in *Proc. Far-IR, Sub-MM, and MM Detector Workshop*, vol. NASA/CP-2003-211 408, J. Wolf, J. Farhoomand, and C. R. McCreight, Eds., 2003, pp. 272–275.
- [7] W. Duncan, W. S. Holland, M. D. Audley, M. Cliffe, T. Hodson, et al., "SCUBA-2: Developing the detectors," in *Proc. SPIE, Millimeter and Submillimeter Detectors for Astronomy*, vol. 4855, T. G. Phillips and J. Zmuidzinas, Eds., Feb. 2003, pp. 19–29.
- [8] J. Gildemeister, A. Lee, and P. Richards, "A fully lithographed voltage-biased superconducting spiderweb bolometer," *Appl. Phys. Lett.*, vol. 74, no. 6, pp. 868–870, 1999.
- [9] D. J. Benford, M. J. Devlin, S. R. Dicker, K. D. Irwin, P. R. Jewell, et al., "A 90 GHz array for Green Bank Telescope, Nuclear Instruments and Methods in Physics Research," *Proc. of the 10th Intern. Workshop on Low Temperature Detectors – LTD-10*, Genoa, Italy, July 7–11, 2003, pp. 387–389.
- [10] J. E. Ruhl, P. A. R. Ade, J. E. Carlstrom et al., "The South Pole Telescope," *Proc. SPIE (Intern. Symp. Astronomical Telescopes)*, 2004 [Online]. Available: www.spt.uchicago.edu/extweb/spt_spie_2004.pdf.
- [11] S. Schwarz and B. Ulrich, "Antenna-coupled IR detectors," *J. Appl. Phys.*, vol. 48, no. 5, pp. 1870–1873, 1977.
- [12] M. Nahum and P. Richards, "Design analysis of a novel low-temperature bolometer," *IEEE Trans. Magn.*, vol. 27, pp. 2484–2487, Mar. 1991.
- [13] J. Mees, M. Nahum, and P. Richards, "New designs for antenna coupled superconducting bolometers," *Appl. Phys. Lett.*, vol. 59, no. 18, pp. 2329–2331, 1991.
- [14] C. L. Hunt, J. J. Bock, P. K. Day, A. Goldin, A. E. Lange, et al., "Transition-edge superconducting antenna-coupled bolometer," in *Proc. SPIE, Millimeter and Submillimeter Detectors for Astronomy*, vol. 4855, T. G. Phillips and J. Zmuidzinas, Eds., Feb. 2003, pp. 318–321.
- [15] M. J. Myers, A. T. Lee, P. L. Richards, D. Schwan, J. T. Skidmore, et al., "Antenna-coupled arrays of voltage-biased superconducting bolometers," in *Proc. 9th Int. Workshop Low Temperature Detectors*, vol. 605, F. S. Porter, D. McCammon, M. Galeazzi, and C. K. Stahle, Eds., 2002, pp. 247–250.
- [16] B. Karasik, W. McGrath, H. LeDuc, and M. Gershenson, "A hot electron direct detector for radioastronomy," *Supercond. Sci. Tech.*, vol. 12, no. 11, pp. 745–747, 1999.
- [17] B. Karasik, W. McGrath, M. Gershenson, and A. Sergeev, "Photon noise-limited direct detector based on disorder-controlled electron heating," *J. Appl. Phys.*, vol. 87, no. 10, pp. 7586–7588, 2000.
- [18] B. S. Karasik, B. Dalaet, W. R. McGrath, J. Weu, M. Gershenson, and A. V. Sergeev, "Experimental study of superconducting hot-electron sensors for submm astronomy," *IEEE Trans. Appl. Supercond.*, vol. 13, pp. 188–191, June 2003.
- [19] A. N. Vystavkin, S. A. Kovtonyuk, A. G. Kovalenko, "Experimental study of superconducting transition in a molybdenum-copper thin film structure showing the proximity phenomenon and the estimation of the sensitivity of TES bolometers on the basis of such a structure," *Nuclear Instruments and Methods in Physics Research*, 2004, vol. A 520, pp. 289–292.
- [20] A. N. Vystavkin, A. V. Pestriakov, "The multiplexing of signals in direct detector arrays using projections method," *Nuclear Instruments and Methods in Physics Research*, 2004, vol. A 520, pp. 562–565.
- [21] G. Chattopadhyay and J. Zmuidzinas, "A dual-polarized slot antenna for millimeter waves," *IEEE Trans. Antennas Propagat.*, vol. 46, pp. 737–737, May 1998.
- [22] J. Yoon, J. Clarke, J. Gildemeister, A. Lee, M. Myers, et al., "Single superconducting quantum interference device multiplexer for arrays of low-temperature sensors," *Appl. Phys. Lett.*, vol. 78, no. 3, pp. 371–373, 2001.
- [23] Microwave Office 2004 Design Suite [Online]. Available: <http://www.appwave.com/products/mwoffice/>
- [24] D. Filipovic, S. Gearhart, and G. Rebeiz, "Double-slot antennas on extended hemispherical and elliptic silicon dielectric lenses," *IEEE Trans. Microwave Theory Tech.*, vol. 41, pp. 1738–1749, Oct. 1993.